

**RELATIONSHIP BETWEEN CHANGE IN LEAF SPRING CAMBER  
AND RESIDUAL STRESSES  
PRODUCED BY SHOT PEENING**

Yoshiaki Kurihara, Masayoshi Shimoseki and Kiyotoshi Sato  
Mitsubishi Steel Mfg. Co., Ltd., Japan

ABSTRACT

An investigation was undertaken to quantitatively determine the relationship between change in leaf spring camber (the camber change) and residual stresses that are set up in leaf spring leaves by shot peening. In the investigation the camber change was analysed as a function of shot peening conditions and the results were verified experimentally. An X-ray analyser was used to measure the distribution of the residual stresses in the direction of leaf thickness. On the basis of the measurement results, a relationship in the form of expressions was derived by the dynamic condition of equilibrium and verified experimentally.

KEYWORDS

shot peening, residual stress, leaf spring camber

## INTRODUCTION

It is widely noted that shot peening raises the leaves' nominal elastic limit and improve fatigue strength. These phenomena are brought about by residual compressive stresses that shot peening set up in the leaves. Such stresses, when set up in an unloaded spring leaf, deform its shape, thus causing the camber of the leaf to change.

One of the key jobs in the manufacturing process of leaf springs is to foresee how much shot peening will change leaf camber. Workers in spring plants have so far relied solely on their own experience to do this job. In order to find a scientific method of predicting the camber change by shot peening, the authors tried to quantitatively determine the relationship between the camber change and the residual stresses that shot peening set up in the leaves.

## ANALYSIS

### Equilibrium Expressions of Internal Stresses in Minute Portions in Longitudinal Direction.

Equilibrium Conditional Expressions. The results of various experiment conducted in the past revealed that residual stresses produced by shot peening performed on one surface of a spring leaf distributed in the direction of the thickness of the leaf as shown by Figure 1. (See References 1, 2 and 3.) They distribute so that the following expressions may hold provided that the resultant of the internal stresses is zero and the angular moment revolving on the neutral axis is also zero:

$$\int_{-T/2}^{T/2} \sigma_x \cdot dx = 0 \quad (1)$$

$$\int_{-T/2}^{T/2} \sigma_x \cdot x \cdot dx = 0 \quad (2)$$

That is, while the residual stresses  $\sigma_x$  should satisfy the dynamical relational expressions (1) and (2), there are infinitely many solutions to the residual stress  $\sigma_x$  which satisfies the expressions (1) and (2). Therefore, a selected value was substituted for  $\sigma_x$  to be solved under the conditions of the expressions (1) and (2) to find its approximate solution.

First, a relational expression among the following was deduced:

- A sine approximation regarded as the most similar to the measured distribution shown in Figure 9.
- The highest of the residual compressive stresses set up in an area adjacent to the peened portion of the leaf which distribute in a shape approximate to a fairly simple rectangle ( $\sigma_1$ ).
- Residual compressive stresses set up in the unpeened portion of the leaf ( $\sigma_2$ ).

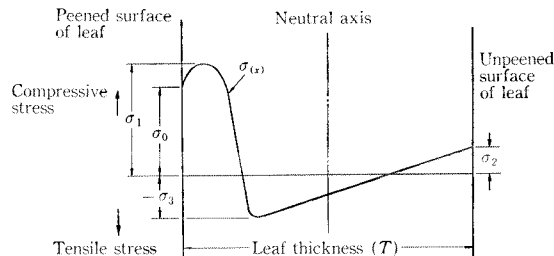


Figure 1 Distribution of Internal Stresses

The following signs are used in the analysis:

$\sigma_0$ : Residual compressive stresses set up in peened portion of leaf (MPa)	$T$ : Leaf thickness (mm)
$\sigma_1$ : Highest of residual compressive stresses set up in area adjacent to peened portion of leaf (MPa)	$E$ : Modulus of longitudinal elasticity (MPa)
$\sigma_2$ : Residual compressive stresses set up in unpeened portion of leaf (MPa)	$\Delta C$ : Amount of camber change (mm)
$\sigma_3$ : Highest of residual tensile stresses set up in area adjacent to peened portion of leaf (MPa)	$\Delta C_A$ : Amount of camber change caused by residual stresses set up in tapered portion of leaf (mm)
$L$ : Leaf span (mm)	$\Delta C_B$ : Amount of camber change shown by tangent angle (mm)
$\rho$ : Curvature radius (mm)	$\Delta C_D$ : Amount of camber change other than that in tapered portion of leaf (mm)
	$\Delta C_T$ : Amount of camber change of leaf with tapered portion (mm)
	$\Delta C_F$ : Amount of camber change of leaf without tapered portion (mm)

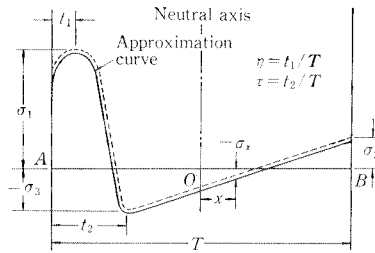


Figure 2 Residual Stress Distribution  
Approximate to Sine Curve

Residual stress distribution approximate to sine curve. The dotted curve in Figure 2 above shows the actual residual stress distribution in a leaf thickness direction which was made when the leaf's side A was shot peened. The solid curve in the figure shows an approximation curve where the internal stress distribution in areas adjacent to the shot peened portion of the leaf was supposed to be a sine curve and that in other areas a straight line. That is, when depth where a residual compressive stress is  $\sigma_1$  is denoted as  $t_1$  and depth where a residual tensile stress is  $\sigma_3$  is represented as  $t_2$ , both of which are measured from side A surface, and an origin is placed on the neutral axis as shown in the figure,  $\sigma_x$  is expressed as follows:

$$\sigma_x = \frac{\sigma_1 + \sigma_3}{2} \sin \left\{ \frac{\pi}{\tau - \eta} \cdot \frac{x}{T} + \frac{\pi(\tau - 3\eta + 1)}{2(\tau - \eta)} \right\} + \frac{\sigma_1 - \sigma_3}{2} \quad (3)$$

where  $-T/2 \leq x \leq -T/2 + t_2$  and  $\eta = t_1/T$ ,  $\tau = t_2/T$

$$\sigma_x = \frac{\sigma_2 + \sigma_3}{1 - \tau} \cdot \frac{x}{T} + \frac{\sigma_2(1 - 2\tau) - \sigma_3}{2(1 - \tau)} \quad (4)$$

where  $-T/2 + t_2 \leq x \leq T/2$  and  $\eta = t_1/T$ ,  $\tau = t_2/T$

Substitution of these two into (1) and (2) gives

$$\int_{-T/2}^{-T/2 + \tau T} \left[ \frac{\sigma_1 + \sigma_3}{2} \sin \left\{ \frac{\pi}{\tau - \eta} \cdot \frac{x}{T} + \frac{\pi(\tau - 3\eta + 1)}{2(\tau - \eta)} \right\} + \frac{\sigma_1 - \sigma_3}{2} \right] dx + \int_{-T/2 + \tau T}^{T/2} \left\{ \frac{\sigma_2 + \sigma_3}{1 - \tau} x + \frac{\sigma_2(1 - 2\tau) - \sigma_3}{2(1 - \tau)} \right\} dx = 0 \quad (5)$$

$$\int_{-T/2}^{-T/2 + \tau T} \left[ \frac{\sigma_1 + \sigma_3}{2} \sin \left\{ \frac{\pi}{2(\tau - \eta)} \left\{ \frac{2x}{T} + (\tau - 3\eta + 1) \right\} + \frac{\sigma_1 - \sigma_3}{2} \right\} \right] x dx + \int_{-T/2 + \tau T}^{T/2} \left[ \frac{\sigma_2 + \sigma_3}{1 - \tau} \cdot \frac{x}{T} + \frac{\sigma_2(1 - 2\tau) - \sigma_3}{2(1 - \tau)} \right] \times x dx = 0 \quad (6)$$

Eliminating  $\sigma_3$  from these two and finding the ratio of  $\sigma_1$  to  $\sigma_2$  :

$$\frac{\sigma_2}{\sigma_1} = -\frac{F(\tau, \eta) \cdot H(\tau, \eta) + G(\tau, \eta) \cdot I(\tau, \eta)}{J(\tau) \cdot H(\tau, \eta) + K(\tau, \eta) \cdot I(\tau, \eta)} \quad (7)$$

$$F(\tau, \eta) = (\tau - \eta) \cos \frac{\pi(\tau - 3\eta)}{2(\tau - \eta)} + \tau\pi$$

$$H(\tau, \eta) = -3\pi(\tau - \eta) \cos \frac{\pi(\tau - 3\eta)}{2(\tau - \eta)} - 6(\tau - \eta)^2 \sin \frac{\pi(\tau - 3\eta)}{2(\tau - \eta)} + (\pi^2 - 6)\tau^2 + \pi^2(1 - 2\tau) + 6\eta(2\tau - \eta)$$

$$G(\tau, \eta) = -3(\tau - \eta)\pi \cos \frac{\pi(\tau - 3\eta)}{2(\tau - \eta)} - 6(\tau - \eta)^2 \sin \frac{\pi(\tau - 3\eta)}{2(\tau - \eta)} - 6(\tau - \eta)^2 + 3\tau\pi^2(\tau - 1)$$

$$I(\tau, \eta) = \pi + (\eta - \tau) \cos \frac{\pi(\tau - 3\eta)}{2(\tau - \eta)}$$

$$J(\tau) = (1 - \tau)\pi$$

$$K(\tau, \eta) = \pi^2(2\tau + 1)(1 - \tau)$$

Now, if the second term is eliminated since  $\tau$  and  $\eta$  are very small amounts, the above can be expressed as:

$$\frac{\sigma_2}{\sigma_1} \approx \frac{X(t_2 - t_1) + t_2\pi}{T \cdot \pi - 2X(t_2 - t_1) - t_2} \quad (8) \quad \text{where} \quad X = \cos \frac{\pi(\tau - 3\eta)}{2(\tau - \eta)}$$

Figure 3 shows the relationship between  $\tau$  and  $\sigma_2/\sigma_1$  based on Expressions (7) and (8) where  $\eta$  is used as a parameter.

By substituting measured values for  $\tau (= t_2/T)$  and  $\eta (= t_1/T)$  (Figure 9) we can easily find the ratio of  $\sigma_1$  to  $\sigma_2$  using these figures. Also,  $\sigma_2$  is found by the substitution of a measured value for  $\sigma_1$ .

Relationship between Curvature Change and Residual Stresses. If shot peening changed the curvature radius of the leaf  $\rho_0$  into  $\rho'$ , the relationship between  $\sigma_2$  and the amount of change in curvature  $(1/\rho_0 - 1/\rho')$  is expressed as:

$$\frac{1}{\rho_0} - \frac{1}{\rho'} = \frac{2\sigma_2}{ET} \quad (9)$$

Substitution of  $\sigma_2$  in Expression (8) into Expression (9) above gives the following expressions to represent the relationship between the amount of change in the curvature and  $\sigma_1$  in residual stress distribution approximate to a sine curve and that approximate to a rectangle, respectively:

$$\frac{1}{\rho_0} - \frac{1}{\rho'} = \frac{2\sigma_1 \{X(t_2 - t_1) + t_2\pi\}}{ET \{T \cdot \pi - 2X(t_2 - t_1) - t_2\}} \quad (10)$$

The above expressions represent the amount of change in the curvature per unit length of the leaf.

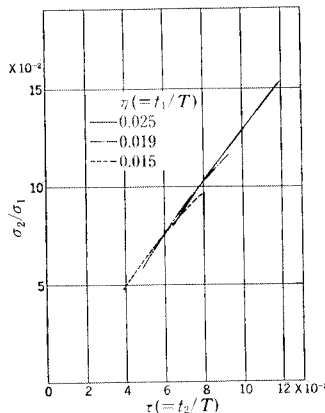


Figure 3  $\sigma_2/\sigma_1$ - $\tau$  diagram by Expression (8)

### Relationship between Camber Change and Change in Curvature.

Since the relationship between the amount of change in the curvature and residual stresses set up by shot peening is obtainable by Expression (10), finding the relationship between the amount of change in the curvature and the amount of the camber change makes it possible for residual stresses to represent the camber change.

Amount of Camber Change of Leaf without Tapered Portion. If shot peening changed the curvature radius  $\rho_0$  into  $\rho'$  and the camber  $C_0$  into  $C'$ , the relationship between the camber and the curvature radius (see Figure 4) is expressed as  $\rho_0 \simeq L^2/8C_0$ ,  $\rho' \simeq L^2/8C'$  for a straight leaf of  $L$  in length. Substitution of them into Expression (9) gives  $\frac{8C'}{L^2} = \frac{8C_0}{L^2} - \frac{2\sigma_2}{ET}$

$$\text{Let } C_0 - C' = \Delta C, \text{ then } \frac{8(C_0 - \Delta C)}{L^2} = \frac{8C_0}{L^2} - \frac{2\sigma_2}{ET}$$

$$\text{Therefore, } \Delta C = \frac{L^2 \sigma_2}{4ET} \quad (11)$$

Thus, the relationship between stresses  $\sigma_2$  set up in unpeened portion of the leaf and  $\Delta C$  is found by Expression (11).

Substitution of Expression (8) into Expression (11) gives

$$\Delta C = \frac{L^2 \{X(t_2 - t_1) + t_2 \pi\} \sigma_1}{4ET \{T \cdot \pi - 2X(t_2 - t_1) - t_2\}} \quad (12)$$

Thus, by using Expression (12) the amount of camber change of a leaf without tapered portion is found as a function of the distribution of internal stresses. These theoretical values will be compared with measured ones in articles for experimental details and results, and discussions.

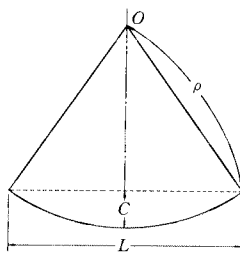


Figure 4 Relationship between camber and curvature radius

Amount of Change in Camber of Leaf with Tapered Portion. Presence of a deflection beam shown in Figure 5 makes it possible to set up the following expressions from a strength of materials point of view. (See Reference 4.)

$$\text{Curvature: } \frac{1}{\rho} = \frac{d^2 C}{dx^2} \quad (13)$$

$$\text{Tangent Angle: } i_2 = \frac{dC}{dx} = - \int_{x_1}^x \frac{1}{\rho} dx + i_1 \quad (14)$$

$$\text{Deflection: } C_2 = \int_{x_1}^{x_2} i dx + C_1 = - \int_{x_1}^{x_2} \int_{x_1}^x \frac{1}{\rho} dx \cdot dx + i_1(x_2 - x_1) + C_1 \quad (15)$$

As Expression (15) shows, the deflection is the double integral of the curvature, which is applicable to the calculation of the amount of camber change of a leaf with a tapered portion. The configuration of the tapered portion is shown by the signs shown in Figure 6:

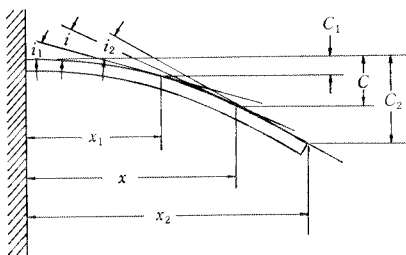


Figure 5 Analytical diagram of deflection beam

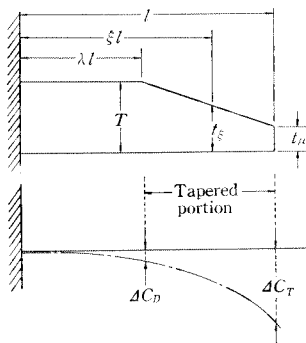


Figure 6 Analyzed tapered portion

By replacing change in leaf thickness by one in leaf length on the basis of Figure 6, we have

$$t_\xi = A + B\xi \quad (16)$$

$$\text{where } A = T(1 - \mu\lambda)/(1 - \lambda), \quad B = T(\mu - 1)/(1 - \lambda)$$

$$l'/l = \lambda (\leq 1), \quad t_\mu/T = \mu (\leq 1)$$

Substitution of Expression (16) into  $T$  in Expression (10) gives

$$d\left(\frac{1}{\rho}\right) = \frac{1}{\rho_0} - \frac{1}{\rho'} = \frac{d}{c\xi^2 + b\xi + a} \quad (17)$$

$$\text{where } a = EA(\pi A - 2Xt_2 + 2Xt_1 - t_2)$$

$$b = EB(2\pi A - 2Xt_2 + 2Xt_1 - t_2)$$

$$c = EB^2\pi$$

$$d = 2\{X(t_2 - t_1) + t_2\pi\}\sigma_1$$

The first term in Expression (15) which represents the relationship between  $\rho$  and  $C$  is expressed as:

$$\begin{aligned} \Delta C_A &= \int_{\lambda}^1 \int_{\lambda}^{\xi} \left( \frac{dl^2}{c\xi^2 + b\xi + a} \right) d\xi \cdot d\xi \\ &= \frac{dl^2}{2c\sqrt{D}} \{-e(\ln e - 1) + g(\ln g - 1) + f(\ln f - 1) - h(\ln h - 1)\} - \frac{dl^2}{\sqrt{D}} (1 - \lambda)(\ln g - \ln h) \end{aligned} \quad (18)$$

The second term in the expression is calculated as follow:

From Figure 7,  $\Delta C_B$  by the deflection angle of the tapered portion is expressed as:

$$\Delta C_B = l\theta(1 - \lambda) \quad (19)$$

Therefore, from Figure 7,  $\theta$  is expressed as:

$$\theta \doteq \frac{2\Delta C_D}{\lambda l} \quad (20)$$

Since  $\Delta C_D$  is found by substituting  $2\lambda l$  into  $L$  in Expression (12).

$$\Delta C_D = \frac{\lambda^2 l^2 \sigma_1 \{X(t_2 - t_1) + t_2\pi\}}{ET\{T \cdot \pi - 2X(t_2 - t_1) - t_2\}}$$

If  $\Delta C_D$  is substituted into Expression (20)

$$\theta = \frac{2\lambda l \sigma_1 \{X(t_2 - t_1) + t_2\pi\}}{ET\{T \cdot \pi - 2X(t_2 - t_1) - t_2\}} \quad (21)$$

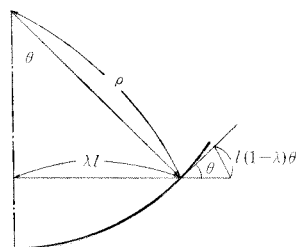


Figure 7 Analytic diagram to find change in camber of tapered portion by tangent angle

Thus,  $\Delta C_B$  is represented by Expression (22) below:

$$\Delta C_B = \frac{2\lambda^2 \sigma_1 (1-\lambda) \{X(t_2-t_1) + t_2\pi\}}{ET\{T\cdot\pi - 2X(t_2-t_1) - t_2\}} \quad (22)$$

Since  $\Delta C_F$  is represented by Expression (12),  $\phi$  which is the ratio of  $\Delta C_T$  to  $\Delta C_F$  is represented by Expression (23) below:

$$\begin{aligned} \phi &= \frac{\Delta C_T}{\Delta C_F} \\ &= \frac{T\{T\cdot\pi - 2X(t_2-t_1) - t_2\}}{B^2\pi\sqrt{D}} \{-e(\ln e - 1) + g(\ln g - 1) + f(\ln f - 1) - h(\ln h - 1)\} \\ &\quad - \frac{2ET\{T\cdot\pi - 2X(t_2-t_1) - t_2\}(1-\lambda)}{\sqrt{D}} \times (\ln g - \ln h) + \lambda(2-\lambda) \end{aligned} \quad (23)$$

where  $A = T(1-\mu\lambda)/(1-\lambda)$ ,  
 $B = T(\mu-1)/(1-\lambda)$ ,  $\mu = t_\mu/T$ ,  $\lambda = l'/l$ ,  
 $a = E\pi A^2 - 2EAX(t_2-t_1) - EA t_2$ ,  
 $b = 2E\pi AB - 2XEB(t_2-t_1) - EB t_2$ ,  
 $c = EB^2\pi$ ,  $d = 2\{X(t_2-t_1) + t_2\pi\}\sigma_1$ ,  
 $e = |b+2c-\sqrt{D}|$ ,  $f = |b+2c+\sqrt{D}|$ ,  
 $g = |b+2c\lambda-\sqrt{D}|$ ,  $h = |b+2c\lambda+\sqrt{D}|$ ,  
 $D = b^2 - 4ac$ ,  $X = \cos\{\pi(t_2-3t_1)/2(t_2-t_1)\}$

The relationship between  $\phi$  and  $\lambda$  which was obtained from Expression (23) is shown in Figure 8.

Let  $\mu = 1$ ,  $\lambda = 1$ , and  $l = L/2$  in Expression (23), then they are Expression (12), by which the camber change of a leaf without tapered portion is calculated. Shown below is a calculation example of  $\Delta C$  of residual stress distribution approximate to a sine curve:

Let  $T = 10$  mm,  $t_1 = 0.15$  mm,  $t_2 = 0.40$  mm,  $\sigma_1 = 657.0$  MPa  
 $l = 500$  mm,  $\mu = 0.5$ ,  $\lambda = 0.1$ , and  $E = 2.059 \times 10^5$  MPa and  
using Expression (18), we have:

$$\Delta C_A = 7.6451 \text{ mm, and}$$

using Expression (19) we have:

$$\Delta C_B = 1.0873 \text{ mm and } \Delta C_D = 0.0004 \text{ mm}$$

Expression (12) gives  $\Delta C_F = 6.0403$  mm,  
therefore,

$$\begin{aligned} \phi &= \frac{\Delta C_A + \Delta C_B + \Delta C_D}{\Delta C_F} \\ &= \frac{7.6451 + 1.0873 + 0.0004}{6.0403} = 1.46 \end{aligned}$$

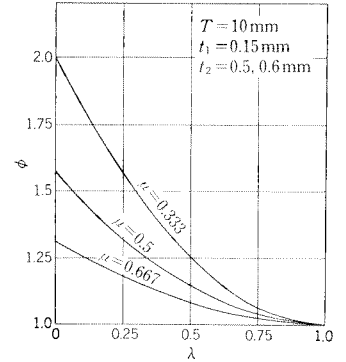


Figure 8  $\phi$ - $\lambda$  diagram

## EXPERIMENTAL DETAILS AND RESULTS

Because of the necessities stated below, we performed experiment to verify the analysis:

- As expressions (12) and (23) show, internal stress distribution such as  $t_1$  and  $t_2$  should be measured to determine the relationship between  $\sigma_1$  and the camber change theoretically.
- It is necessary to measure  $\Delta C$  before and after shot peening to compare the theoretical relationship between the amount of the camber change and shot peening degree with measured one.
- Theoretically obtained  $\Delta C$  of both a leaf with camber and one without camber should be compared with  $\Delta C$  obtained in measurement.

Experimental Details

Table 1 Description of Test Specimens

Dimension (mm)*	Steel Grade	Hardness (HB)	Shot Peening Type
6 x 70 x 600	JIS SUP 9	363 - 415	Regular
8 x 70 x 600	JIS SUP 9	363 - 415	Regular
10 x 70 x 600	JIS SUP 9	363 - 415	Regular
6 x 70 x 1000	JIS SUP 9	363 - 415	Regular
8 x 70 x 1000	JIS SUP 9	363 - 415	Regular
10 x 70 x 1000	JIS SUP 9	363 - 415	Regular

- Notes: \*Dimension: Thickness x Width x Length
- 1. The specimen group of each dimension comprises a cambered leaf and an uncambered one.  
(Camber : 80 mm)
  - 2. All the specimens are without tapered portions.

In order to investigate the effect of shot peening on the specimens, Almen arc height was measured and then residual stress distribution in the direction of leaf thickness and  $\Delta C$  were measured with an X-ray analyzer after shot peening which had been performed under the following conditions:  
Type of shot peening machine: Centrifugal peening type  
Shot type and size: Cut wire 0.8 mm in diameter  
Arc height (mm A): 0.405/0.495/0.585  
Coverage: 90% or more

Measurement of Residual Stress Distribution with X-ray Analyzer.

Alternate electrolytic polishing to a depth of approximately 0.05 mm of the 40-mm-thick specimens and measurement of residual stresses in the longitudinal direction thereof with X-ray were repeated (Figure 9). Figure 9 shows measured stress distribution after correction of the effect of the electrolytic polishing. (See References 5 and 6.) Table 2 below shows the conditions under which the polishing and the measurement were performed:

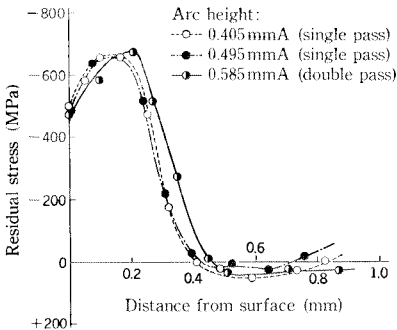


Figure 9 Measured stress distribution

Table 2 Conditions for Electrolytic Polishing and X-ray Measurement

Type of X-ray Measurement	Regular type
Target	CrK $\alpha$
Voltage	30 KV
Count Full Scale	2,000 - 4,000 cps
Time Constant	4 sec.
Soller Slits	0.68°
Mask	4 mm
Voltage for Polishing	15 V
Current	2 A
Solution	Ammonium chloride + Water + Glysline



Measurement Results of Camber Change.

$\Delta C$  of the specimens before and after shot peening was measured with a dial gauge, the results of which are shown in Figures 10, 11, and 12 below:

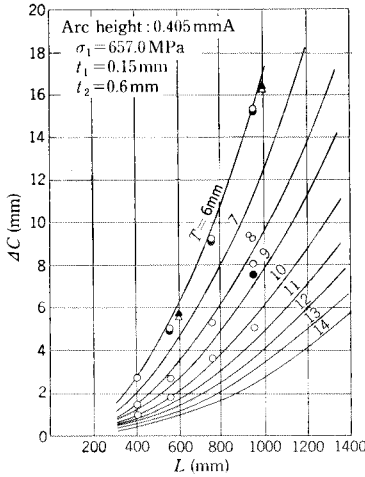


Figure 10  $\Delta C$ - $L$  diagram

- : Measured  $\Delta C$  of uncambered leaf
- : Corrected  $\Delta C$  of uncambered leaf
- △ : Measured  $\Delta C$  of cambered leaf
- ▲ : Corrected  $\Delta C$  of cambered leaf
- : Theoretical curve

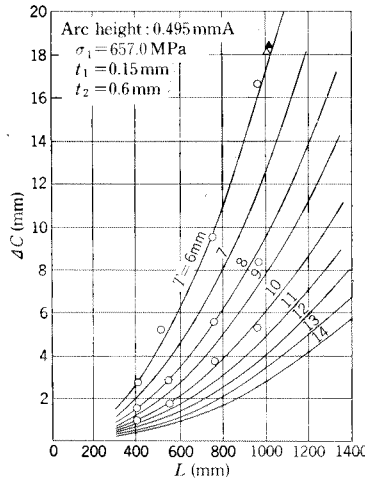


Figure 11  $\Delta C$ - $L$  diagram

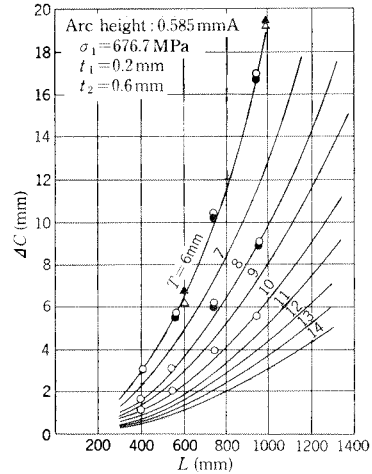


Figure 12  $\Delta C$ - $L$  diagram

DISCUSSION

The results of our residual stresses measurement are shown in Figure 9. The analysis of the results show that the number of pass hardly change stresses set up in the neighborhood of leaf surface ( $\sigma_0$  and  $\sigma_1$ ), but  $t_1$  of  $\sigma_1$ . In order to obtain  $\Delta C$ ,  $\sigma_1$ ,  $t_1$ , and  $t_2$  readings are taken from Figure 9, then  $\sigma_2$  is found by Figure 4. The relationship between  $L$  and  $\Delta C$  is obtained by the substitution of  $\sigma_2$  into Expression (11). As can be seen from Figures 10, 11, and 12, the theoretical residual stress distribution approximate to a sine curve has great similarity to the measurements. However, in the calculation of  $\Delta C$  of largely cambered leaves  $L$  in Expression (11) should be considered as their arc length. Such consideration was made to obtain the corrected values shown in the figures.

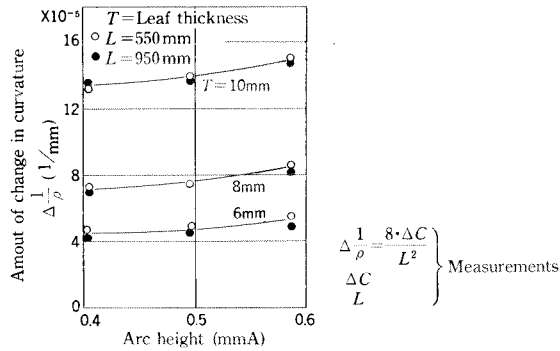


Figure 13  $\Delta(1/\rho)$  Arc height diagram

Figure 8 shows the ratio of the camber change of leaves with tapered portions to that of ones without them in the residual stress distribution approximate to a sine curve.

In the calculation of  $\Delta C$  of regular leaf springs with tapered portions of  $\lambda = 1.0 \sim 0.8$  and  $\mu = 0.5 \sim 0.3$ , the portions are believed to be negligible, but in the case of ones with long-tapered portions they must be included in the calculation.

Figure 13 shows the relationship between arc height and change in leaf curvature. As can be seen from it, arc height variation between 0.405 and 0.585 mm A causes the curvature to change between 1 and  $2 \times 10^{-5}$  (1/mm).

## CONCLUSION

The analysis of the results of the investigation reveals that:

- A sinusoidal approximation is the accurate analyzing method of residual stress distribution.
- The amount of the camber change of leaf springs without tapered portions can be obtained as a function of shot peening conditions and leaf thickness.
- The above are true of both straight and curved spring leaves. The arc length of the curved leaves is required to be considered as leaf length.
- In the calculation of the camber change amount of springs with tapered portions, such portions are negligible unless they are long ones.

## REFERENCES

- (1) The Wheelabrator Corp., "Shot Peening in Spring Design", 1966
- (2) The Wheelabrator Corp., Shot Peening, Vol. 8, p. 131, 1965
- (3) Society of Spring Research, Japan, Spring (Revised 3rd ed.), p. 348, 1970
- (4) Udoguchi, Kawada, and Kuranishi, Material Strength, p. 214, 1975
- (5) Aoyama, Namikawa, and Iwanaga, "Material" Vol. 17, p. 1083, 1956
- (6) Kawada and Watanabe, "Material Testing" Vol. 5, p. 497, 1956
- (7) Kamishobara, "Machinery" p. 1023, 1963
- (8) Kodama, "Journal of the Japan Society of Mechanical Engineers" Vol. 75, p. 1026, 1972